LETTER

doi:10.1038/nature16502

Lithium–ion battery structure that self–heats at low temperatures

Chao–Yang Wang[1,2], Guangsheng Zhang[1], Shanhai Ge[2], Terrence Xu[2], Yan Ji[2], Xiao–Guang Yang[1] & Yongjun Leng[1]

Lithium-ion batteries suffer severe power loss at temperatures below zero degrees Celsius, limiting their use in applications such as electric cars in cold climates and high-altitude drones[1,2]. The practical consequences of such power loss are the need for larger, more expensive battery packs to perform engine cold cranking, slow charging in cold weather, restricted regenerative braking, and reduction of vehicle cruise range by as much as 40 per cent[3]. Previous attempts to improve the low-temperature performance of lithium-ion batteries[4] have focused on developing additives to improve the low-temperature behaviour of electrolytes[5,6], and on externally heating and insulating the cells[7–9]. Here we report a lithium-ion battery structure, the 'all-climate battery' cell, that heats itself up from below zero degrees Celsius without requiring external heating devices or electrolyte additives. The self-heating mechanism creates an electrochemical interface that is favourable for high discharge/charge power. We show that the internal warm-up of such a cell to zero degrees Celsius occurs within 20 seconds at minus 20 degrees Celsius and within 30 seconds at minus 30 degrees Celsius, consuming only 3.8 per cent and 5.5 per cent of cell capacity, respectively. The self-heated all-climate battery cell yields a discharge/regeneration power of 1,061/1,425 watts per kilogram at a 50 per cent state of charge and at minus 30 degrees Celsius, delivering 6.4–12.3 times the power of state-of-the-art lithium-ion cells. We expect the all-climate battery to enable engine stop–start technology capable of saving 5–10 per cent of the fuel for 80 million new vehicles manufactured every year[10]. Given that only a small fraction of the battery energy is used for self-heating, we envisage that the all-climate battery cell may also prove useful for plug-in electric vehicles, robotics and space exploration applications.

Figure 1a schematically shows a generic lithium (Li)-ion all-climate battery (ACB) cell. In addition to the three essential battery components—anode, cathode and electrolyte—we add here a fourth component: a nickel (Ni) foil 50 μm in thickness having two tabs, one at each end. Electrical resistance between the two tabs is designed to be 56 mΩ at room temperature (25 °C) to keep the cell voltage around 2 V and to avoid solid–electrolyte interphase decomposition and copper foil oxidation. One tab is electrically connected to the negative terminal, welded together with the tabs of all anode layers. The second tab of the Ni foil extends outside the cell to form a third terminal, the activation terminal, used to activate battery internal heating at low temperatures. A switch connects the activation terminal with the negative terminal. When the switch is left open during cell activation for self-heating, electrons must flow through the Ni foil, generating substantial ohmic heat, which rapidly warms up the core of the battery. Once the battery internal temperature reaches or exceeds 0 °C, thereby enabling the electrochemical interface to generate high power for both discharge and charge, the activation process is completed and the switch is closed. When the ACB cell operates at around room temperature, the switch between the activation terminal and negative terminal remains closed, making electrons bypass the Ni foil and reverting the ACB cell to a conventional Li-ion cell with very low internal resistance and high power. The switch between activation terminal and negative terminal may be controlled by the cell surface temperature.

Figure 1b shows cell voltage and surface temperature evolutions during cell activation followed by a 1C discharge of a 7.5 amp-hour (Ah) ACB cell at −20 °C, and similar results are shown in Extended Data Fig. 1a and b for −30 °C and −40 °C, respectively. The cell exhibits sufficiently high voltage to stay 'healthy' (that is, the battery materials do not suffer potential degradation) throughout activation and 1C discharge processes even from as low as −40 °C. More noteworthy is that the cell surface temperature rises rapidly, in seconds, from an extremely cold environment to 0 °C within the activation process (better seen in the insets to Fig. 1b and Extended Data Fig. 1, where the cell activation process is magnified). It is clear that cell activation takes only 19.5 s, 29.6 s and 42.5 s from environments at −20 °C, −30 °C and −40 °C, respectively. After activation, the cell surface temperature drops slightly below the freezing point owing to large heat loss to the cold surroundings in these environmental-chamber tests; however, in reality it would remain around the freezing point owing to the thermal insulation usually applied around cells. The 1C discharge energy, calculated by integrating the area underneath each discharge curve, is 102 watt-hours per kilogram (Wh kg^{-1}) for the ACB cell at −40 °C, compared to only 0.3 Wh kg^{-1} for the baseline cell without Ni foil. The ACB cell thus provides much more usable energy, enabling a longer cruising range for an electric car, especially in extreme cold.

The ultrafast cell activation discovered in this work makes ACB cells technologically viable for boosting battery power. Fundamentally, the activation time may be estimated as follows. Assuming negligible heat loss from cell surfaces to the surroundings owing to a short time duration (this assumption is realistic as batteries are well insulated in vehicles), the energy balance during cell activation is:

$$\int_0^{\tau_{act}} I_{act}(U_0 - V_{act})\mathrm{d}t = mc_p\Delta T \quad (1)$$

where I_{act} and V_{act} are current and output voltage during cell activation, U_0 is the thermal equilibrium potential of a Li-ion cell (~4.2 V for the cells used in this study), τ_{act} is activation time, m is cell mass, c_p is the specific heat of the cell, and ΔT is the rise in temperature from the initial ambient temperature to, for example, 0 °C. Assuming $c_p = 1{,}000\ \mathrm{J\,kg^{-1}\,K^{-1}}$ and using an average activation current I_{act} of 47.4 A in the −30 °C activation case (see Extended Data Fig. 2), the theoretical activation time τ_{act} is estimated to be 26.7 s, very close to the measured 29.6 s. This also indicates that the self-heating mechanism devised in the ACB cell structure is very energy-efficient (~90% in this case). If $V_{act} = 0$ V activation is implemented, one can convert 10% more electric energy into internal heat for battery warm-up from very low temperatures, thereby further shortening activation time. This is the greatest advantage of ACB cells over existing battery heating methods, which are much more energy- and time-consuming[7–9]. For example,

[1]Department of Mechanical and Nuclear Engineering and Electrochemical Engine Center (ECEC), The Pennsylvania State University, University Park, Pennsylvania 16802, USA. [2]EC Power, 341 Science Park Road, State College, Pennsylvania 16803, USA.

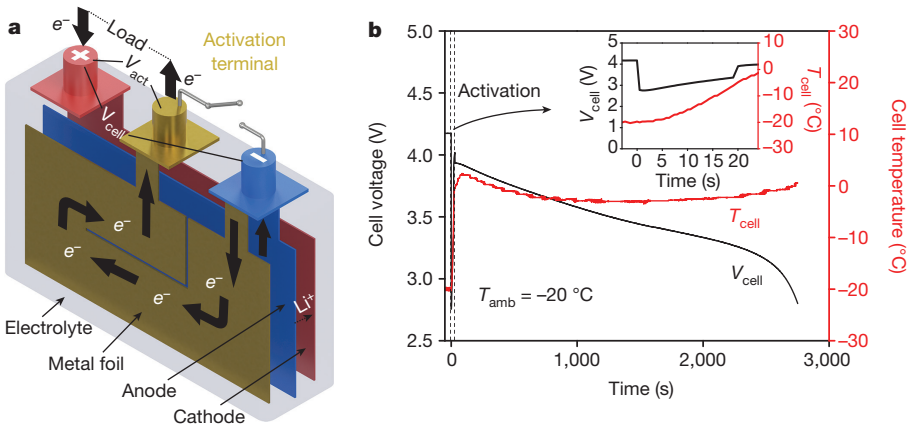

Figure 1 | The ACB. a, Schematic in which a metal foil is inserted to generate internal heating from a low temperature and to provide fast heat transfer to electrodes and electrolyte. This self-heating function is activated by turning off the switch between the activation terminal and the negative terminal. **b**, Cell voltage and temperature evolutions during V_{act} = 0.4 V activation (inset) and subsequent 1C discharge at −20 °C. The battery temperature rises from −20 °C to 0 °C in ~20 s and the 1C discharge thereafter occurs at the ~0 °C battery core temperature rather than the −20 °C ambient temperature.

Vlahinos and Pesaran[7] computationally showed that battery core heating based on the cell's internal resistance is more effective than external heating methods. Stuart and Handeb[8] argued that direct-current internal heating is ineffective and instead implemented expensive, heavy alternating-current generators for heating. More recently, Ji and Wang[9] thoroughly reviewed a wide range of heating strategies for Li-ion batteries and demonstrated that self-resistive heating from −20 °C to 20 °C takes ~120 s and consumes ~15% battery energy. For heating from −20 °C to 0 °C as in the present context, their cell would require a 60-s heating time and 7.5% energy consumption, much less efficient than the present ACB cell.

Another important feature of the ACB cell is high power, immediately available after ultrafast activation just as the battery materials and electrochemical interfaces reach 0 °C. In Fig. 2a, for −20 °C, −30 °C and −40 °C, a 10-s hybrid pulse power characterization (HPPC) power in watts per kilogram, for both discharge and regeneration (charge), as a function of depth of discharge is compared to that of a conventional Li-ion cell without Ni foil. At 50% state-of-charge (SOC) or depth of discharge, the power boost over the conventional Li-ion cell is 2.7, 6.4 and 25.1 for −20 °C, −30 °C and −40 °C, respectively, for discharge, and 5.1, 12.3 and 55 for regeneration. Figure 2b plots the specific power versus ambient

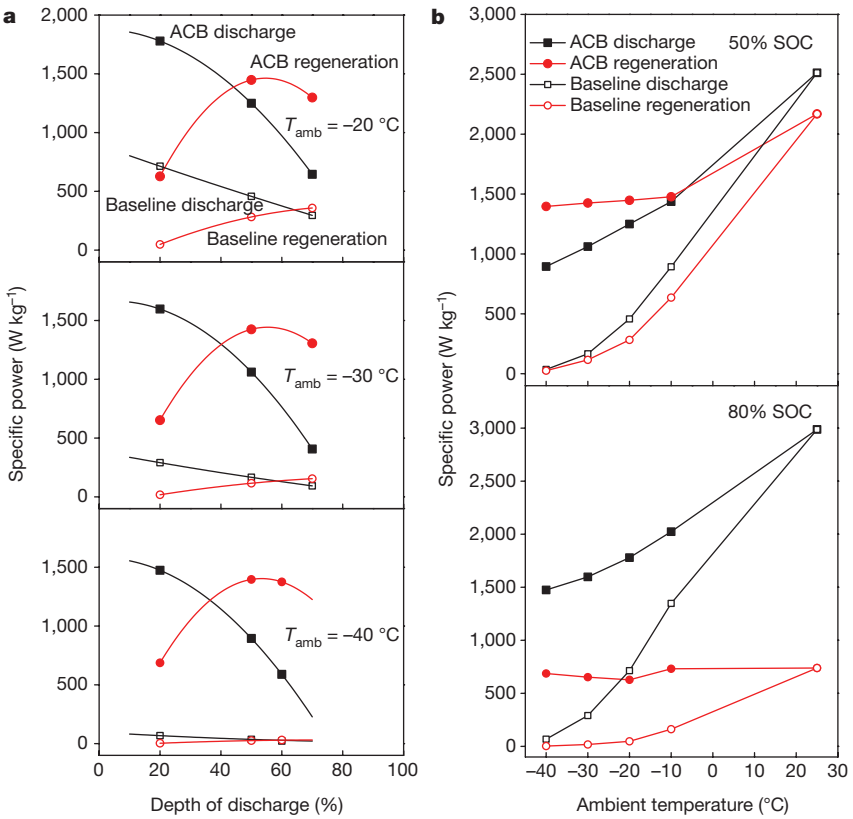

Figure 2 | Power performance of the ACB cell. a, 10-s HPPC specific power versus depth of discharge, compared to the baseline cell for −20 °C, −30 °C and −40 °C. At 50% SOC, the ACB cell delivers 2.7 times, 6.4 times and 25.1 times the discharge power and 5.1 times, 12.3 times and 55 times the regeneration power of a baseline cell at −20 °C, −30 °C and −40 °C, respectively. **b**, 10-s HPPC specific power after activation versus the baseline as function of ambient temperature for 50% and 80% SOC.

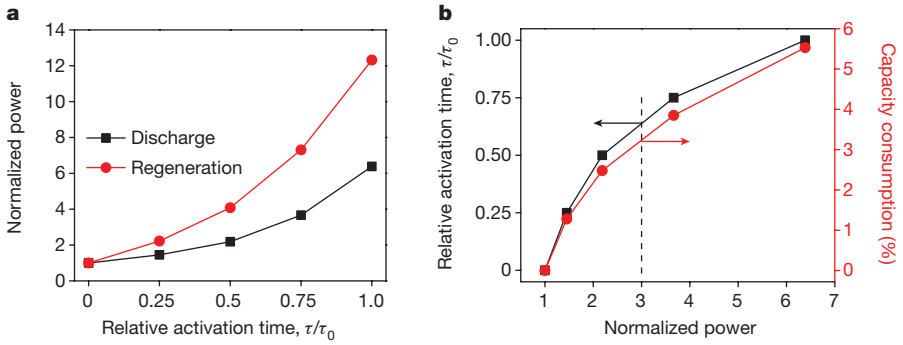

Figure 3 | Power on demand at 50% SOC for 10-s HPPC at −30 °C. **a**, Normalized power (ACB/baseline) versus relative activation time. τ_0 is the time of full activation. **b**, Relative activation time and percentage capacity consumption due to activation as functions of normalized power. 5.5% energy (the right *y*-axis) can be exchanged, on demand, for 640% power (the *x*-axis), or 3.2% energy can be exchanged for 300% power.

temperature for both ACB and baseline cells at 50% and 80% SOC, respectively. The discharge power (black lines in Fig. 2b) of the ACB cell is improved to 1,061 W kg^{-1} and 1,600 W kg^{-1} at −30 °C for 50% and 80% SOC, respectively. These power levels are more than 5–6 times the power of the baseline Li-ion cell at the same temperature. Regeneration power at low temperatures is equally impressive for the ACB cell, reaching 1,425 W kg^{-1} at 50% SOC and 650 W kg^{-1} at 80% SOC at −30 °C, indicative of unprecedented high charge/regeneration power in the extreme cold. These high power capabilities, readily available after a short activation, open new possibilities for a wide variety of applications where high battery power is critically sought. A few examples are the expedient capture of braking energy in extreme cold where it is most needed, weather-independent fast charging, and high-flying drones at low atmospheric temperatures.

For ACB cells to enjoy a dramatic power boost at low temperatures, some activation time and energy (or charge) consumption are required. Both can be further managed by exercising a power-on-demand strategy, that is, implementing partial activation to attain a smaller but sufficient power boost. Such experiments are shown in Fig. 3a and b under the conditions of −30 °C and 50% SOC, where normalized power, that is, the power of the ACB cell over the baseline, is plotted against the relative activation time. Obviously, for zero activation time or no activation at all, the normalized power is unity. At 100% activation, the normalized power for the ACB cell at −30 °C reaches 6.4 times the discharge power and 12.3 times the regeneration power, respectively. However, at a partial activation such as 50%, there are already marked increases in both discharge and regeneration power, as can be seen from Fig. 3a. Figure 3b re-plots the relative activation time and capacity consumption percentage due to activation against the normalized power. It is seen that for a 3-fold power boost, 66% partial activation suffices and the capacity consumption due to cell activation is only 3.2% for heating from the ambient temperature of −30 °C. Therefore, the power-on-demand strategy further reduces the activation time from 30 s to 20 s and also the capacity consumption due to activation from 5.5% to 3.2%, at the expense of having 3-fold power instead of 6.4-fold power.

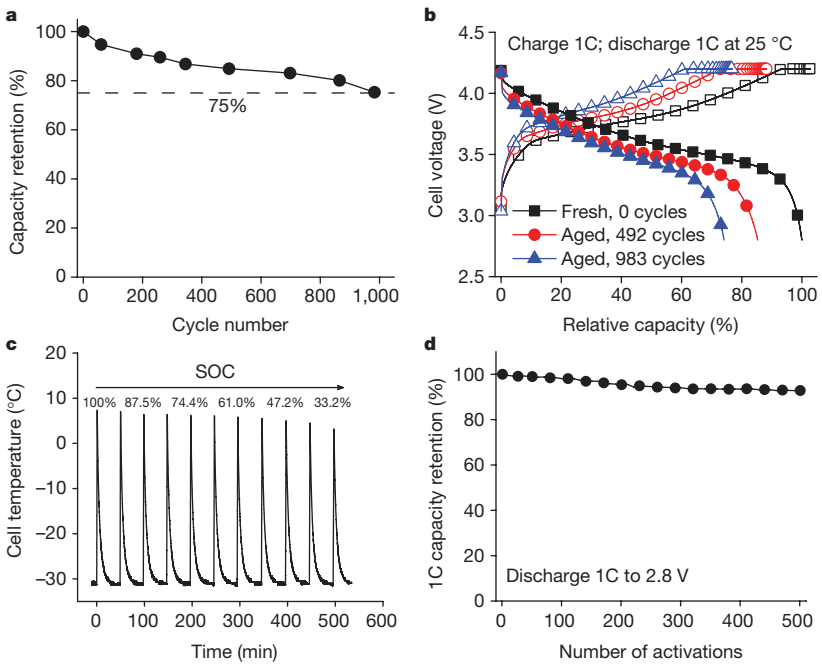

Figure 4 | ACB cell durability. **a**, C/3 capacity retention. In the present context, C/3 = (7.5 A)/3 = 2.5 A discharge current. **b**, 1C charge/discharge curves of fresh cells and cells aged from 45 °C cycling between 2.8 V and 4.15 V. Both capacity retention and charge/discharge curves in **a** and **b** are obtained during cell characterization at 25 °C. ACB cells give rise to almost no side effects in high-temperature cycling. **c**, Cell surface temperature versus time in a series of ten consecutive cycles of activation and cool-down in durability of repetitive activations from T_{amb} = −30 °C. The change in SOC during the ten cycles is also indicated. **d**, 1C capacity versus number of activations for T_{amb} = 25 °C. The constant-current, constant-voltage charge protocol is constant current at 1C followed by constant voltage at 4.2 V and terminated when the charge current diminishes to C/20. Little degradation exists, even after 500 activations from −30 °C.

To project a further large reduction in activation time, τ_{act}, and capacity consumption, Q_{act}/Q_o, for future energy-dense electric-vehicle batteries, it follows from equation (1) that if the C-rate, β (which is the dimensionless electric current, relative to the cell capacity, such that in the present context, 1C for a 7.5-Ah cell is equivalent to a discharge current of 7.5 A), during activation is kept constant, the activation time and percentage capacity consumption are proportional to:

$$\tau_{act} = \frac{mc_p\Delta T}{Q_0(U_0 - V_{act})\beta} \propto \frac{\overline{V}}{U_0 - V_{act}}\frac{1}{\rho_e} \quad (2)$$

$$\frac{Q_{act}}{Q_0} = \frac{mc_p\Delta T}{Q_0(U_0 - V_{act})} \propto \frac{\overline{V}}{U_0 - V_{act}}\frac{1}{\rho_e} \quad (3)$$

where ρ_e is the cell's energy density and $\overline{V}$ is the nominal voltage used in calculating the energy density.

Note that both activation time and capacity consumption will drop by half if the energy density is doubled from the current level of 170 Wh kg^{-1} to a future level of 340 Wh kg^{-1}. The halved activation time and capacity consumption would be at levels of ~10 s and 1.9% for ACB cell activation from −20 °C, a common low-temperature environment. Further implementing a partial activation based on power demand, it would be possible to keep the ACB activation time within 5 s and capacity consumption within 1%, while still delivering sufficient power for a wide range of applications involving cold climates.

Existing techniques improve low-temperature power at the expense of greatly deteriorated performance and lifespan at high temperatures. Figure 4a and b shows no additional side effects with high-temperature cycling, and a normal 17% loss of capacity with room-temperature cycling over 2,000 cycles (Extended Data Fig. 3).

Finally, we explore cell degradation caused by repetitively activating an ACB cell from −30 °C followed by forced air cool-down. A consecutive ten cycles of activation and cool-down is carried out for an ACB cell, starting with 100% SOC (Fig. 4c). Thereafter, the cell is charged back to 100% SOC at room temperature and with standard constant-current, constant-voltage protocol having a voltage limit of 4.2 V. A total of 500 such activations are carried out, and the cell capacity at room temperature and 1C rate characterized at the end of every ten activation/cool-down cycles is shown in Fig. 4d. The cell capacity fade is less than 7.2% at the end of 500 activations. In a practical electric-vehicle battery pack, once all batteries are heated to a higher temperature, the cool-down timescale usually ranges from several hours to 10–15 h. This implies that cell activation is probably only needed once per day. Assuming 30 days of extreme weather (−30 °C) per year, 500 activations tested in the durability experiment shown in Fig. 4d would be equivalent to about 16 years of operation, meaning battery life is not noticeably decreased by cell activation from subfreezing temperatures.

The new material we added into the baseline battery to make it an ACB cell—that is, the Ni foil—weighs about 100 g per kilowatt-hour battery and costs US$0.1 per kilowatt-hour based upon a Ni price of US$10 per kilogram. Compared to the current best specific energy of Li-ion battery systems, which is 150 Wh per kilogram of the battery system, and assuming a battery cost of US$250 per kilowatt-hour (ref. 11), the added weight and cost due to ACB technology are 1.5% and 0.04% of those of the baseline battery.

Online Content Methods, along with any additional Extended Data display items and Source Data, are available in the online version of the paper; references unique to these sections appear only in the online paper.

Received 20 September; accepted 30 November 2015.
Published online 20 January 2016.

1. Armand, M. & Tarascon, J. M. Building better batteries. *Nature* **451,** 652–657 (2008).
2. Villasenor, J. High-altitude surveillance drones: coming to a sky near you. *Sci. Am.* **Feb**, 24 (2012).
3. Extreme temperatures affect electric vehicle driving range, AAA says. http://newsroom.aaa.com/2014/03/extreme-temperatures-affect-electric-vehicle-driving-range-aaa-says/ *Newsroom* (20 March 2014).
4. Ji, Y., Zhang, Y. & Wang, C. Y. Li-ion cell operation at low temperatures. *J. Electrochem. Soc.* **160,** A636–A649 (2013).
5. Zhang, S. S., Xu, K. & Jow, T. R. A new approach toward improved low temperature performance of Li-ion battery. *Electrochem. Commun.* **4,** 928–932 (2002).
6. Smart, M. C., Whitacre, J. F., Ratnakumar, B. V. & Amine, K. Electrochemical performance and kinetics of $Li_{1+x}(Co_{1/3}Ni_{1/3}Mn_{1/3})_{1-x}O_2$ cathodes and graphite anodes in low-temperature electrolytes. *J. Power Sources* **168,** 501–508 (2007).
7. Vlahinos, A. & Pesaran, A. A. Energy efficient battery heating in cold climates. Society of Automotive Engineers (SAE) Technical Paper 2002–01–1975, http://papers.sae.org/2002-01-1975/ (SAE, 2002).
8. Stuart, T. A. & Handeb, A. HEV battery heating using AC currents. *J. Power Sources* **129,** 368–378 (2004).
9. Ji, Y. & Wang, C. Y. Heating strategies for Li-ion batteries operated from subzero temperatures. *Electrochim. Acta* **107,** 664–674 (2013).
10. Chen, K. *et al.* Evaluation of the low temperature performance of lithium manganese oxide/lithium titanate lithium-ion batteries for start/stop applications. *J. Power Sources* **278,** 411–419 (2015).
11. Gröger, O., Gasteiger, H. A. & Suchsland, J.-P. Electromobility: batteries or fuel cells? *J. Electrochem. Soc.* **162,** A2605–A2622 (2015).

Acknowledgements We thank W. Zhao and C. E. Shaffer for early discussions on using battery simulation software to discover the all-climate battery. This work was inspired by US patent publication numbers 2014-0342194, 2015-0303444 and 2015-0104681 and Patent Cooperation Treaty publication numbers WO 2014/186195, WO 2015/102709 and WO 2015/102708.

Author Contributions C.Y.W. developed the concept and wrote the manuscript. S.G., T.X., Y. J. and X.G.Y. designed and built the cells, G.Z. built the test stand and carried out the performance characterization, and Y.L. performed the cycle life experiments. All authors contributed to development of the manuscript and to discussions as the project developed.

Author Information Reprints and permissions information is available at www.nature.com/reprints. The authors declare competing financial interests: details are available in the online version of the paper. Readers are welcome to comment on the online version of the paper. Correspondence and requests for materials should be addressed to C.Y.W. (cxw31@psu.edu or cywang@ecpowergroup.com).

METHODS

We fabricate 7.5-Ah ACB pouch cells using $LiNi_{0.5}Co_{0.2}Mn_{0.3}O_2$ (Umicore) as cathodes and graphite (Nippon Carbon) as anodes with 1 M of $LiPF_6$ dissolved in ethylene carbonate/ethyl methyl carbonate (3:7 by weight) + 2% vinylene carbonate as electrolyte (materials from BASF). The capacity ratio of negative to positive electrode is designed to be 1.2. The 7.5-Ah pouch cell contains a stack of 26 anode and 25 cathode layers. A Celgard-2325 separator of thickness 25 μm is used. A Ni foil sized at 56 mΩ at room temperature is coated with a thin backing material of polyethylene terephthalate (28 μm) for electrical insulation and sandwiched between two single-sided anode layers and the three-layer assembly then stacked in the centre of the cell.

The cathodes are prepared by coating *N*-methylpyrrolidone-based slurry onto 15-μm-thick Al foil, whose dry material consists of NCM523 (92 wt%), Super-P (Timcal) (4 wt%) and polyvinylidene fluoride (Arkema) (4 wt%) as a binder. The anodes are prepared by coating deionized water-based slurry onto 10-μm-thick Cu foil, whose dry material consists of graphite (97.5 wt%), styrene butadiene rubber (Zeon) (1.5 wt%) and carboxymethyl cellulose (Dai-Ichi Kogyo Seiyaku) (1 wt%).

Each ACB pouch cell has a 152 mm × 75 mm footprint area, weighs 160 g, and has a nominal capacity of 7.5 Ah with a specific energy of 170 Wh kg^{-1} and an energy density of 327 Wh per litre. The discharge performance of the ACB cell at room temperature without activation is shown in Extended Data Fig. 4 as a function of the C-rate.

We denote the voltage between the positive and negative terminals as cell voltage, a potential window encompassing all battery materials. Additionally, we denote the voltage between the positive and activation terminals as V_{act} for the activation process only. For any subzero operation, cell activation is first carried out by a constant-voltage, constant-current protocol where constant voltage means that V_{act} is set at 0.4 V until the current reaches and is limited at 60 A (that is, 8C). Cell activation is terminated when the cell temperature reaches −5 °C as measured by a thermocouple placed at the centre of the cell's outer surface. A 10-s rest is given between the end of activation and cell loading for equilibrium, during which the cell surface temperature usually continues to rise to 0 °C. Hence, cell activation described in the present work is designed to bring the battery core temperature to or above the freezing point from any subzero ambient environment. Prior to any subfreezing tests, an ACB cell is soaked in the environmental chamber for 8–12 h to reach thermal equilibrium with the ambient temperature.

Two types of cell discharge are performed in the present work. One is 1C discharge with a cutoff voltage of 2.8 V and the other is 10-s HPPC in which at a given SOC level, a 10-s charge pulse is applied at $V_{max} = 4.2$ V, followed by a 40-s rest and a discharge pulse at $V_{min} = 2.8$ V. The discharge and charge (or regeneration) power, in watts per kilogram of the battery cell is calculated as the product of constant voltage and average current in the 10-s discharge and charge pulses, then divided by the cell weight.

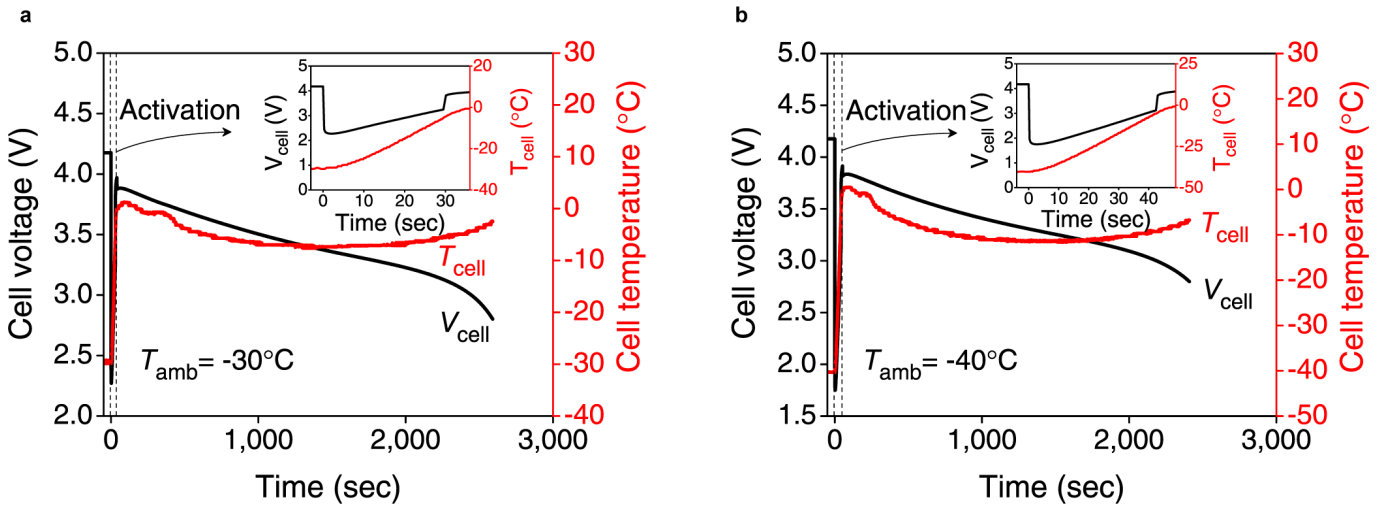

Extended Data Figure 1 | Cell voltage and temperature evolution during activation and subsequent 1C discharge. a, −30 °C. **b**, −40 °C. The insets show the $V_{act} = 0.4$ V activation more clearly.

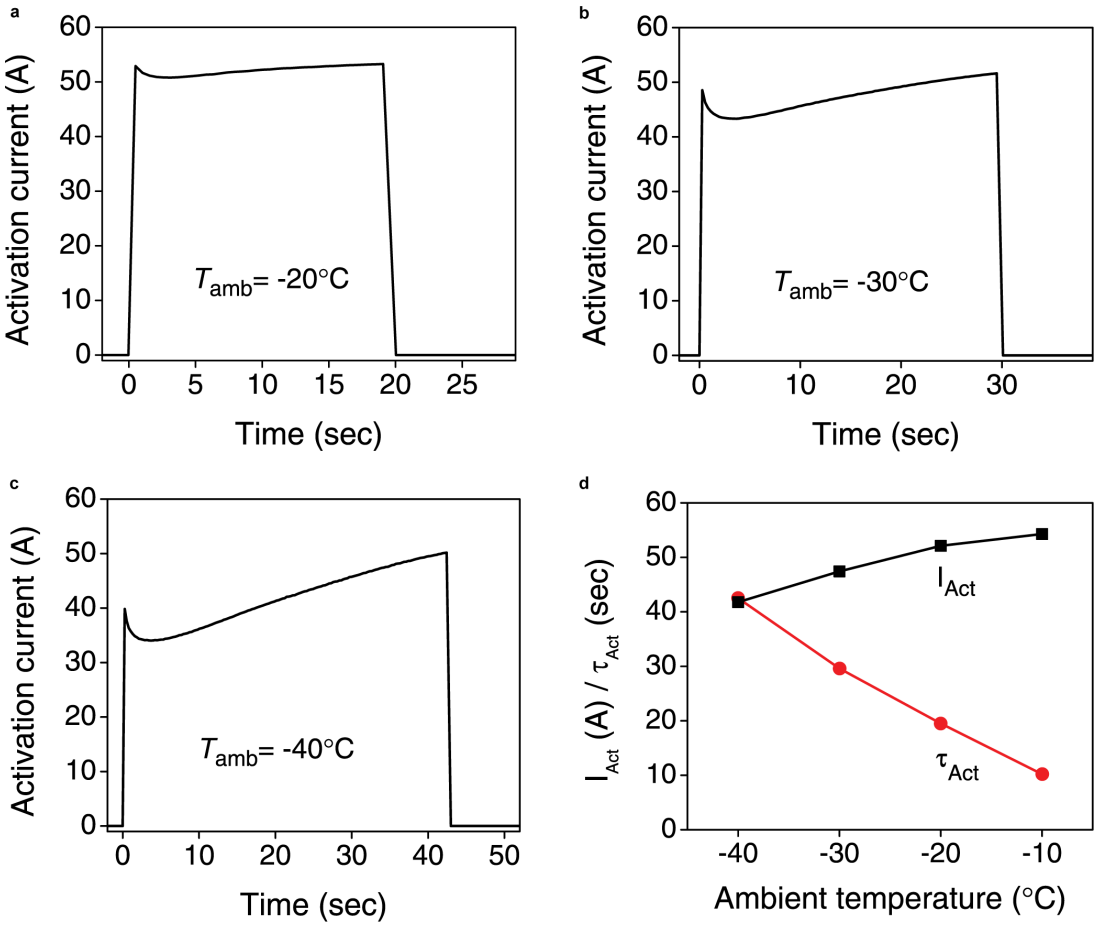

Extended Data Figure 2 | Cell current variations during activation. a, −20 °C. **b**, −30 °C. **c**, −40 °C. **d**, Activation time τ_{act} and average activation current I_{act} versus the ambient temperature T_{amb}.

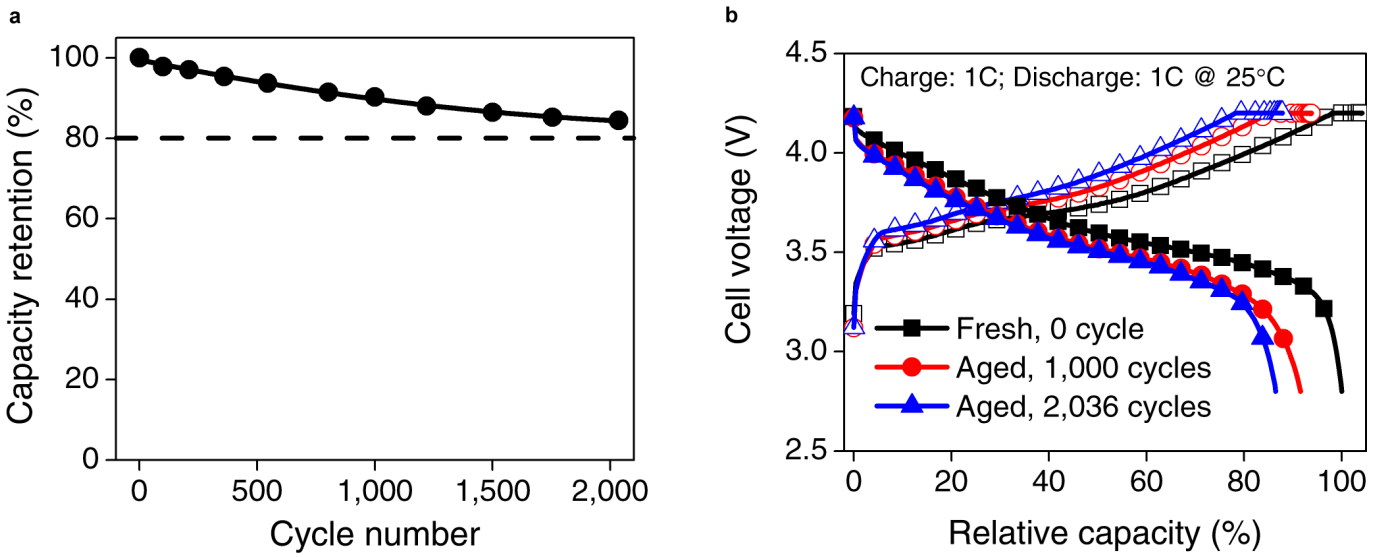

Extended Data Figure 3 | 1C charge/2C discharge cycling of ACB cell at room temperature between 2.8 V and 4.2 V. a, C/3 capacity retention. **b**, 1C charge/discharge curves of the fresh and aged cells.

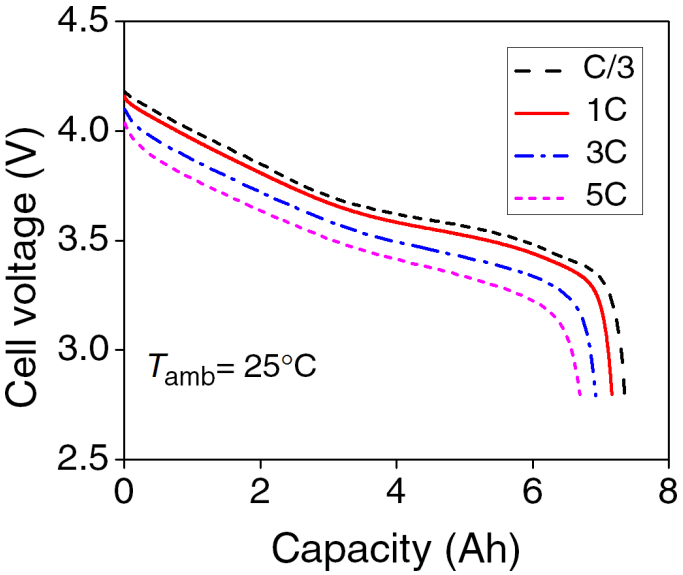

Extended Data Figure 4 | ACB cell discharge with various C-rates of discharge and at room temperature.